Reducing the frequency of the Higgs mode in a helical superconductor coupled to an LC circuit

Yao Lu,[1,*] Stefan Ilić,[1] Risto Ojajärvi,[2] Tero T. Heikkilä,[3,†] and F. Sebastian Bergeret[1,4,‡]

[1]*Centro de Física de Materiales (CFM-MPC), Centro Mixto CSIC-UPV/EHU, Manuel de Lardizabal 5, E-20018 San Sebastián, Spain*

[2]*Institute for Theory of Condensed Matter, Karlsruhe Institute of Technology (KIT), 76131 Karlsruhe, Germany*

[3]*Department of Physics and Nanoscience Center, University of Jyväskylä, P.O. Box 35 (YFL), FI-40014 University of Jyvaskyla, Finland*

[4]*Donostia International Physics Center (DIPC), Manuel de Lardizabal 4, E-20018 San Sebastián, Spain*

(Received 26 December 2022; accepted 6 December 2023; published 26 December 2023)

We show that the amplitude or Higgs mode of a superconductor with strong spin-orbit coupling and an exchange field, couples linearly to the electromagnetic field. Furthermore, by coupling such a superconductor to an LC resonator, we demonstrate that the Higgs resonance becomes a regular mode at frequencies smaller than the quasiparticle energy threshold $2\Delta_0$. We finally propose and discuss a possible experiment based on microwave spectroscopy for an unequivocal detection of the Higgs mode. Our approach may allow visualizing Higgs modes also in more complicated multiband superconductors with a coupling between the charge and other electronic degrees of freedom.

DOI: 10.1103/PhysRevB.108.224517

Introduction. In superconductors with spontaneously broken $U(1)$ symmetry, the Higgs mode is an excitation associated with the oscillation of the order parameter amplitude around its saddle point value [1–5]; see Fig. 1. Despite the progress in studying the Higgs mode in systems where charge-density-wave order and superconductivity coexist [5–9], or via its nonlinear coupling to the electromagnetic (EM) field [10–21], detecting unequivocally the Higgs mode, in general, remains a challenging task.

One of the obstacles is that the Higgs mode in conventional superconductors is a scalar mode, and hence it couples nonlinearly to the EM field. A linear coupling can be achieved in the presence of a supercurrent [22]. A second reason for its challenging detection is that with a mass of $2\Delta_0$, the Higgs mode resides precisely at the bottom of the quasiparticle continuum, and is thus overdamped by the quasiparticle excitations. Unlike a regular collective mode, the Higgs mode corresponds to a square root singularity of the pair susceptibility. As a result, it decays in time in a power law fashion $\delta\Delta(t) \sim \delta\Delta(0)\cos(2\Delta_0 t)/\sqrt{2\Delta_0 t}$ [23], where $\delta\Delta$ is a small perturbation of the pairing gap around its average value, Δ_0. Even though it was suggested that the mass of the Higgs mode can be below the energy gap in strongly disordered superconductors [24], it was shown later that in such systems, the Higgs mode never shows up as a real mode [25].

In this paper, we propose a way of overcoming these difficulties. We first demonstrate that the amplitude mode in helical superconductors [26–28] couples linearly to the EM field, even in the absence of a supercurrent. Helical superconductivity occurs in systems where both inversion and time-reversal symmetries are broken, for instance due to magnetic fields and spin-orbit coupling (SOC). Second, we exploit such a linear coupling and demonstrate the reduction of the Higgs frequency by coupling the superconductor to an LC resonator (Fig. 1). When the resonant frequency of the LC mode is slightly larger than the Higgs frequency, and the direct coupling between the two modes is finite, they repel each other, and the Higgs mode is pushed down to frequencies smaller than $2\Delta_0$ making it a well-defined mode.

Summary of the results from a phenomenological model. In a conventional superconductor the Higgs-light coupling is characterized by the susceptibility

$$\chi_{A\Delta} = \frac{\partial^2 S}{\partial \boldsymbol{A}\partial\Delta} = \frac{\partial \boldsymbol{J}}{\partial\Delta}, \tag{1}$$

where S is the action, $\boldsymbol{A}$ is the vector potential, and $\boldsymbol{J} = \partial S/\partial \boldsymbol{A}$ is the supercurrent. Near the critical temperature, $\boldsymbol{J} \propto \Delta^2$, and the susceptibility is $\chi_{A\Delta} \propto J/\Delta$. In other words, it is finite only in the presence of a supercurrent [22].

The situation is different in superconductors with broken time-reversal and inversion symmetries. These may correspond to superconductors with Rashba SOC and an in-plane exchange field, intensively studied in the context of magnetoelectric phenomena in superconductors, such as helical superconductivity [26–28], Josephson ϕ_0 junctions [29,30], and most recently supercurrent diode effects [31–36]. In this case, the action up to the fourth order in the order parameter is given by [35,36]

$$S = S_0 + \int dt d\boldsymbol{r}(\boldsymbol{a}_1\tilde{\boldsymbol{Q}} + b_1\tilde{\boldsymbol{Q}}^2)|\Delta(t)|^2 + (\boldsymbol{a}_2\tilde{\boldsymbol{Q}} + b_2\tilde{\boldsymbol{Q}}^2)|\Delta(t)|^4, \tag{2}$$

where $\tilde{\boldsymbol{Q}} = \boldsymbol{Q} + \boldsymbol{A}(t)$ is the gauge-invariant condensate momentum and $\boldsymbol{Q}$ is the phase gradient of the order parameter. S_0 is the zeroth-order term in $\tilde{\boldsymbol{Q}}$, and $\Delta(t)$ the time-dependent

*yao.lu@ehu.eus
†tero.t.heikkila@jyu.fi
‡fs.bergeret@csic.es

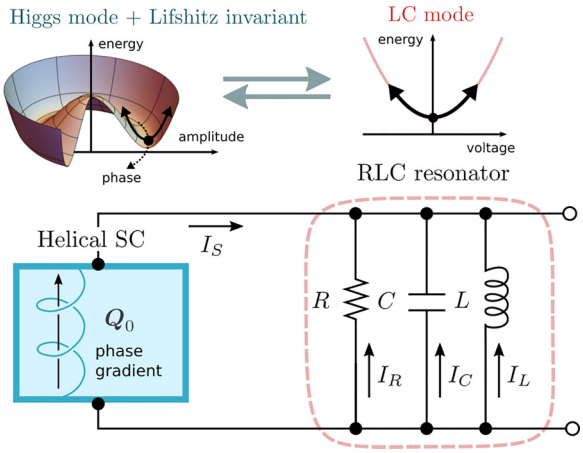

FIG. 1. Schematic diagram of the circuit that couples a helical superconductor and an LC resonator. Microwave is sent to the system through a transmission line, and the resonance modes are detected by measuring the microwave reflection rate. The Lifshitz invariant couples the supercurrent and the Higgs mode.

order parameter $\Delta(t) = \Delta_0 + \delta\Delta(t)$. The constants $b_{1,2}$ are the usual Ginzburg-Landau (GL) coefficients appearing in even-power terms of $\tilde{\boldsymbol{Q}}$. Linear-in-$\tilde{\boldsymbol{Q}}$ terms, $\boldsymbol{a}_1$ and $\boldsymbol{a}_2$, are only allowed in superconductors with broken time-reversal and inversion symmetries, and are related to the Lifshitz invariant [37,38,39].

The action, Eq. (2), describes a helical superconductor with a spatially varying order parameter in the ground state, $\Delta(\boldsymbol{r}) = \Delta_0 e^{i\boldsymbol{Q}_0\boldsymbol{r}}$ [26–28]. The amplitude of modulation $\boldsymbol{Q}_0$ can be determined from the condition that the supercurrent $\boldsymbol{J}$ in the ground state must vanish: $\partial S/\partial \boldsymbol{Q}|_{\boldsymbol{Q}=\boldsymbol{Q}_0} = 0$. Thus, $\boldsymbol{Q}_0 = -(\boldsymbol{a}_1 + \boldsymbol{a}_2\Delta_0^2)/[2(b_1 + b_2\Delta_0^2)]$. Next, we calculate $\chi_{\boldsymbol{A}\Delta}$ by taking $\boldsymbol{Q} = \boldsymbol{Q}_0 + \delta\boldsymbol{Q}$, where $\delta\boldsymbol{Q}$ is a phase gradient generated by passing a supercurrent through the system. Substituting Eq. (2) into Eq. (1) we obtain the Higgs-light coupling

$$\chi_{\boldsymbol{A}\Delta} = \int d\boldsymbol{r}\left(4\Delta_0\delta\boldsymbol{Q}(b_1 + 2b_2\Delta_0^2) + \frac{2(\boldsymbol{a}_2 b_1 - \boldsymbol{a}_1 b_2)\Delta_0^3}{b_1 + b_2\Delta_0^2}\right). \tag{3}$$

The first term describes the linear Higgs-light coupling due to a finite supercurrent discussed above and established in Ref. [22]. The second term is an additional contribution that is only finite in helical superconductors for which $\boldsymbol{a}_1$ and $\boldsymbol{a}_2$ are nonzero. Equation (3) suggests that helical superconductors can potentially exhibit a linear Higgs-light coupling, even without the presence of an applied supercurrent. The rest of the paper is dedicated to demonstrating, within a microscopic model, the conditions under which this statement holds true. Additionally, we show how the Higgs mode would be affected if it were linearly coupled to an LC resonator. In writing Eq. (3) we use the stationary version of the GL theory because it is simple and gives us qualitatively an idea about the origin of Higgs-light coupling. But, we note that this theory is limited and fails to capture the vanishing Higgs-light coupling in the clean case, as we show using the microscopic theory.

Let us now investigate how the structure of the Higgs mode would change, if it were to be coupled linearly to an LC resonator (see setup in Fig. 1). The Higgs mode is described by the fluctuations of the order parameter $\delta\Delta(t)$, whereas the LC mode is described by the time-varying voltage $V(t)$. In frequency domain, the effective equations of motion of this system can be written as

$$\begin{pmatrix} \sqrt{\Omega_H - \Omega + i\Gamma_H} & \gamma_1 \\ \gamma_2 & \Omega_0 - \Omega + i\Gamma_0 \end{pmatrix}\begin{pmatrix} \delta\Delta(\Omega) \\ V(\Omega) \end{pmatrix} = 0. \tag{4}$$

Here Ω_H and Ω_0 are the resonant frequencies of the Higgs and the LC mode, respectively, and Γ_H and Γ_0 are the damping parameters. The coupling coefficients γ_1 and γ_2 are proportional to $\chi_{\boldsymbol{A}\Delta}$. We assume a vanishing injected DC supercurrent, which is why only the second term in Eq. (3) contributes to the coupling.

In the absence of any coupling, $\gamma_1 = \gamma_2 = 0$, the Higgs mode is not a well-defined mode with a Lorentzian line shape, as reflected in the square root function in Eq. (4). On the other hand, the LC mode is a regular mode. For a finite but small coupling such that $\Gamma_H \ll \mathrm{Re}(\eta^2) \ll \Omega_0 - \Omega_H$, where $\eta = \gamma_1\gamma_2/(\Omega_0 - \Omega_H + i\Gamma_0)$, and a low dissipation of the LC mode, $\Gamma_0 < \Omega_0 - \Omega_H$, we can approximate the eigenvalue equation near the Higgs frequency as

$$\sqrt{\Omega_H - \Omega + i\Gamma_H} - \eta = 0. \tag{5}$$

If $\mathrm{Re}(\eta) > 0$, the eigenvalue equation can be linearized around the new resonance frequency and becomes

$$[\Omega_H - \mathrm{Re}(\eta^2) - \Omega] + i[\Gamma_H - \mathrm{Im}(\eta^2)] = 0. \tag{6}$$

The Higgs mode is shifted away from the branch cut at Ω_H to a lower frequency $\Omega_H - \mathrm{Re}(\eta^2)$, and becomes a real mode with a potentially small linewidth $\Gamma_H - \mathrm{Im}(\eta^2)$ [40]. Thus by coupling the two modes, the resonant response from the Higgs mode can be dramatically enhanced and its frequency reduced. This is our second main result. In what follows we derive our findings from a microscopic model.

Microscopic theory. One realization of helical superconductivity is a quasi-two-dimensional superconductor with strong Rashba SOC and an in-plane magnetic field. To calculate the susceptibility $\chi_{\boldsymbol{A}\Delta}$, we start with the generalized Eilenberger equation describing this system in the basis of the two helical bands labeled by the index $\lambda = \pm 1$ [41,42]:

$$\begin{aligned} &i\boldsymbol{n}\cdot(\boldsymbol{Q}v_F/2 + \lambda\boldsymbol{h}_{\mathrm{ex}}\times\hat{z})[\tau_3, \hat{g}_{\lambda\boldsymbol{n}}] - \{\partial_t\tau_3, \hat{g}_{\lambda\boldsymbol{n}}\} \\ &\quad = [\Delta_0\tau_1 + \Delta_\Omega e^{-i\Omega t}\tau_1 + \hat{\Sigma}_{\lambda\boldsymbol{n}}, \hat{g}_{\lambda\boldsymbol{n}}]. \end{aligned} \tag{7}$$

Here, $\hat{g}_{\lambda\boldsymbol{n}}$ is the quasiclassical Green function of the band λ with the momentum direction at the Fermi level given by $\boldsymbol{n} = \boldsymbol{p}/p_F$. It is a matrix in the Nambu space, spanned by the Pauli matrices $\tau_{1,2,3}$ and the identity matrix 1. The normalization condition $\hat{g}_{\lambda\boldsymbol{n}}^2 = 1$ holds. $\boldsymbol{Q}$ is the phase gradient of the order parameter, $\boldsymbol{h}_{\mathrm{ex}}$ is the exchange field, and $\hat{z}$ is the unit vector perpendicular to the plane of the superconductor. v_F is the Fermi velocity, Δ_0 is the saddle point value of the order parameter, and Δ_Ω is the Fourier amplitude of the external pairing potential with frequency Ω. $\hat{\Sigma}_{\lambda\boldsymbol{n}}$ is the disorder self-energy

$$\hat{\Sigma}_{\lambda\boldsymbol{n}} = \sum_{\lambda'}\frac{1}{4\tau_{\lambda'}}(\langle\hat{g}_{\lambda'\boldsymbol{n}'}\rangle_{\boldsymbol{n}'} + \lambda\lambda'\boldsymbol{n}\cdot\langle\boldsymbol{n}'\hat{g}_{\lambda'\boldsymbol{n}'}\rangle_{\boldsymbol{n}'}). \tag{8}$$

Here τ_λ is the effective scattering time for the band λ, $\frac{1}{\tau_\lambda} = \frac{1}{\tau}(1 + \lambda\frac{\alpha}{v_F})$, where τ is the impurity scattering time. α is the velocity associated with Rashba SOC. Note that Eq. (7) is valid when SOC is larger than all other energy scales except the chemical potential μ, namely $\mu \gtrsim \alpha p_F \gg \Delta, h_{ex}, \tau^{-1}, Qv_F, T$, where T is the temperature. In the absence of disorder, the two bands are decoupled, but share the same order parameter. Disorder couples the bands by introducing interband scattering.

Within linear response to the external field, the Green function can be written as $\hat{g} = \hat{g}^{(0)}e^{i\omega(t_1-t_2)} + \hat{g}^{(\Delta)}e^{i\omega_1 t_1 - i\omega_2 t_2}$, with $\omega_1 = \omega$ and $\omega_2 = \omega + \Omega$. Here $\hat{g}^{(0)}$ is the unperturbative static Green function and $\hat{g}^{(\Delta)}$ denotes the external field-induced dynamical Green function, which is of the first order in Δ_Ω. Once we solve the Eilenberger equation, the supercurrent can be determined from

$$\boldsymbol{J}^{(0,\Delta)} = \sum_\lambda N_\lambda v_F \mathrm{Tr}\big[\tau_3 \big\langle \boldsymbol{n}\hat{g}^{(0,\Delta)}_{\lambda\boldsymbol{n}}\big\rangle_{\boldsymbol{n}}\big]. \tag{9}$$

Here, $\boldsymbol{J}^{(0)}$ and $\boldsymbol{J}^{(\Delta)}$ correspond to DC and AC supercurrents, respectively. $N_\lambda = N_0(1 + \lambda\frac{\alpha}{v_F})$ is the density of states of band λ, with N_0 denoting the average density of states. From the condition $\boldsymbol{J}^{(0)}(\boldsymbol{Q} = \boldsymbol{Q}_0) = 0$, we first determine the modulation vector of the helical superconductivity $\boldsymbol{Q}_0$. Finally, we calculate $\chi_{\boldsymbol{A}\Delta}$ from

$$\chi_{\boldsymbol{A}\Delta} = \boldsymbol{J}^{(\Delta)}/\Delta_\Omega. \tag{10}$$

Our method using the Eilenberger equation is equivalent to the diagrammatic approach taking into account all the ladder impurity diagrams as explained in Ref. [13].

First, we consider $\chi_{\boldsymbol{A}\Delta}$ in two limiting cases, namely, the pure ballistic and the diffusive limits. In the ballistic limit $\tau^{-1} \to 0$, the system preserves a Galilean symmetry [43,44], so that the current is time independent despite the presence of an external pairing field, and hence $\chi_{\boldsymbol{A}\Delta} = 0$. On the other hand, in the diffusive limit $\tau^{-1} \gg \Delta, T$, the two helical bands are strongly mixed by disorder, and both bands are described by the same Usadel equation derived in Ref. [41]. This leads to $\chi_{\boldsymbol{A}\Delta} = 0$ (see the Supplemental Material [42]).

For intermediate degree of disorder one needs to solve the Eilenberger equation, Eq. (7). The weak exchange field allows for an analytic solution presented in the Supplemental Material [42,45]. We find a nonmonotonic behavior of $\chi_{\boldsymbol{A}\Delta}$ while increasing the disorder strength [Fig. 2(a)]. Without the disorder potential, $\chi_{\boldsymbol{A}\Delta}$ is zero, consistent with the above symmetry analysis. With increasing disorder strength, $\chi_{\boldsymbol{A}\Delta}$ rapidly reaches its maximum and then decays as a power law. We also verified that $\chi_{\boldsymbol{A}\Delta}$ vanishes in the diffusive limit, when $1/\tau\Delta_0 \gg 1$. In this work, we focus on the case where the Fermi energy is much greater than any other energy scale $E_F \gg \Delta_0, 1/\tau, T$. This is a totally different parameter regime from those considered in Refs. [46–49], where E_F is comparable with Δ_0 and $1/\tau$.

The linear Higgs-light coupling leads to a modification of the admittance of the superconductor. To find the total admittance, we write the order parameter as $\Delta = \Delta_0 + \delta\Delta(t)$ and expand the action up to the second order in $\delta\Delta$ and the external field $\boldsymbol{A}$, $S = S_M + S_f$, where S_M is the mean-field term and S_f is the fluctuation term given by

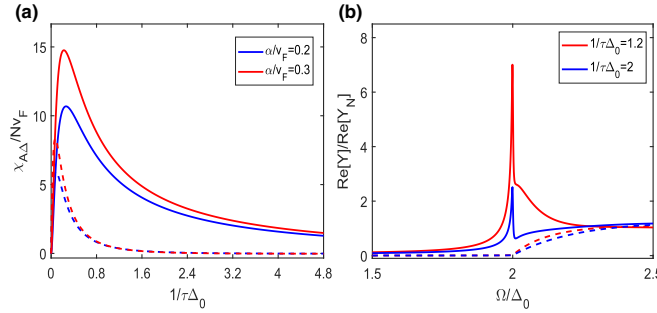

FIG. 2. (a) Real part (solid lines) and imaginary part (dashed lines) of $\chi_{A\Delta}$ at $\Omega = 2\Delta_0$ as a function of the disorder strength for different strengths of spin-orbit coupling. $\chi_{A\Delta}$ behaves nonmonotonically as a function of the disorder strength. (b) The real parts of admittance normalized by its value in the normal state with (solid line) and without (dashed line) the Higgs contribution. The peak localized at $\Omega = 2\Delta_0$ is the signature of the Higgs mode. The parameters used here are $T = 0.1\Delta_0$, $h_{\mathrm{ex}}/\Delta_0 = 0.5$. In panel (b), $\alpha/v_F = 0.3$. The Dynes parameter is $\Gamma = 0.001\Delta_0$.

$$S_f = \frac{1}{T}\sum_n \begin{bmatrix} \delta\Delta(-\Omega_n) \\ \boldsymbol{A}(-\Omega_n) \end{bmatrix}^{\mathsf{T}} \begin{bmatrix} -\chi^{-1}_{\Delta\Delta} & \chi_{\Delta\boldsymbol{A}} \\ \chi_{\boldsymbol{A}\Delta} & \chi_{\boldsymbol{AA}} \end{bmatrix} \begin{bmatrix} \delta\Delta(\Omega_n) \\ \boldsymbol{A}(\Omega_n) \end{bmatrix}, \tag{11}$$

where Ω_n is the bosonic Matsubara frequency $\Omega_n = 2n\pi T$ with $n \in \mathbb{Z}$. $\chi_{\Delta\boldsymbol{A}}$ is defined in Eq. (10), whereas $\chi_{\Delta\Delta}$ and $\chi_{\Delta\boldsymbol{A}}$ are defined as $\chi_{\Delta\boldsymbol{A}} = \partial F/\partial\boldsymbol{A}$, and $\chi_{\Delta\Delta} = \partial F/\partial\Delta_\Omega - 1/U$, where F is the pair correlation $F = \sum_\lambda N_\lambda \mathrm{Tr}[\tau_1\langle\hat{g}_{\lambda\boldsymbol{n}}\rangle_{\boldsymbol{n}}]$ and U is the BCS interaction. $\chi_{\Delta\boldsymbol{A}}$ and $\chi_{\boldsymbol{A}\Delta}$ are related by $\chi_{\Delta\boldsymbol{A}}(\Omega) = \chi_{\boldsymbol{A}\Delta}(-\Omega)^* = \chi_{\boldsymbol{A}\Delta}(\Omega)$ [50]. Finally, the field susceptibility is defined as $\chi_{\boldsymbol{AA}} = \partial\boldsymbol{J}/\partial\boldsymbol{A}$.

The pair susceptibility $\chi_{\Delta\Delta}$ has a square root singularity at $\Omega = 2\Delta_0$ indicating the existence of the Higgs mode. Integrating out the $\delta\Delta$ field, we obtain the total field susceptibility

$$\tilde{\chi}_{\boldsymbol{AA}} = \chi_{\boldsymbol{AA}} + \chi_{\boldsymbol{A}\Delta}\chi_{\Delta\Delta}\chi_{\Delta\boldsymbol{A}}, \tag{12}$$

which defines the total admittance $Y = \tilde{\chi}_{\boldsymbol{AA}}/i\Omega$. Here the first term $\chi_{\boldsymbol{AA}}$ represents the conventional AC response of the superconductor, whereas the second term is the Higgs contribution to the AC response. When $\chi_{\boldsymbol{A}\Delta}$ and $\chi_{\Delta\boldsymbol{A}}$ are finite, the admittance exhibits a peak at the Higgs frequency [Fig. 2(b)] providing a way of detecting the Higgs mode using standard experimental methods.

To couple the Higgs mode with an LC resonator we consider the circuit shown in Fig. 1. A capacitor and an inductor form an LC resonator. The effect of the conventional conductance of the superconductor is only to modify the inductance and resistance of the LC loop as explained in the Supplemental Material [42]. The total inductance of the circuit, $L^{-1}_{\mathrm{tot}} = L^{-1} + L_S^{-1}$, includes the inductance L of the LC resonator and the kinetic inductance of the superconductor $L_S = 1/\mathrm{Re}[\chi_{AA}]$. The total resistance is $R^{-1}_{\mathrm{tot}} = R^{-1} + R_S^{-1}$, where R represents the damping of the LC circuit and R_S is the resistance of the superconductor given by $R_S = i\Omega/\mathrm{Im}[\chi_{\boldsymbol{AA}}]$. We propose an experiment in which microwaves are sent to the system, for example through a transmission line, whereas the complex reflection coefficient is measured. To explicitly calculate the

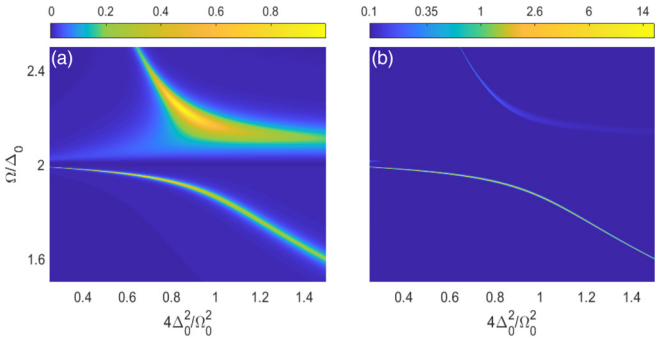

FIG. 3. (a) The microwave absorption rate W and (b) the modified pair susceptibility $\chi^m_{\Delta\Delta}$ as functions of the inductance L and the frequency Ω. Here we have assumed that the resistance is dominated by the resistance of the superconductor $R = R_S$. The parameters used here are $T = 0.1\Delta_0$, $\frac{1}{\tau\Delta_0} = 0.4$, $\frac{h_{ex}}{\Delta_0} = 0.5$, $\frac{\alpha}{v_F} = 0.3$, $C = \frac{E_F}{2\Delta_0^2}\frac{e_0^2}{2\pi}$, $Z_t = 100\frac{\Delta_0}{E_F}\frac{h}{e_0^2}$, where E_F is the Fermi energy of the superconductor. Here we restore the electron charge e_0 and the Planck constant h for clarity. The Dynes parameter is $\Gamma = 0.001\Delta_0$.

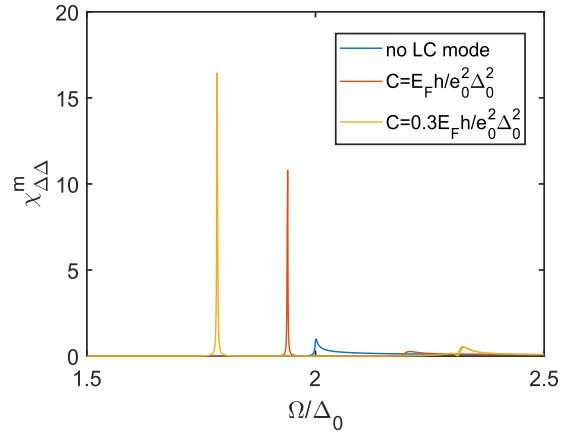

FIG. 4. The modified pair susceptibility $\chi^m_{\Delta\Delta}$ as a function of frequency for different values of C normalized by the maximum value without the LC resonator. The frequency of the LC resonator is fixed $\Omega_0 = \frac{1}{\sqrt{L_{tot}C}} = 2.1\Delta_0$. The parameters used here are the same as those in Fig. 3.

modified Higgs spectrum, we combine the equation of current conservation $I_C + I_R + I_L + I_S = I_{ext}$, and the self-consistency equation for the dynamical part of the order parameter [42]

$$\hat{M}\begin{pmatrix}\delta\Delta(\Omega)\\ V(\Omega)/id\Omega\end{pmatrix} = \begin{pmatrix}0\\ I_{ext}/Cd\end{pmatrix}, \tag{13}$$

with the response matrix given by

$$\hat{M} = \begin{pmatrix}\chi^{-1}_{\Delta\Delta} & -\chi_{A\Delta}\\ -\chi_{\Delta A}\Omega_0 Z_0 & \Omega^2 - \Omega_0^2 - i\Omega\kappa\end{pmatrix}, \tag{14}$$

where $\Omega_0 = \sqrt{1/L_{tot}C}$, $Z_0 = \sqrt{L_{tot}/C}$, $\kappa = 1/R_{tot}C$, and d is the size of the superconductor. The analytical expression of $\chi_{\Delta\Delta}$ was obtained in Ref. [5]. Its general form is complicated, but for $\Omega \lesssim 2\Delta_0$, $\chi^{-1}_{\Delta\Delta}$ scales as $\sqrt{2\Delta_0 - \Omega}$. The system can thus be effectively described by Eq. (4). Moreover, when $\Omega < \Omega_H = 2\Delta_0$, $\chi_{A\Delta} = \chi_{\Delta A}$ become real [42]. The resonance frequency is determined by $\det\hat{M} = 0$. The total impedance of the system is given by

$$Z = \left[i\Omega C + \frac{1}{i\Omega L} + \frac{1}{R} + \frac{\tilde{\chi}_{AA}}{i\Omega}\right]^{-1}, \tag{15}$$

which determines the microwave reflection rate $r = (Z - Z_t)/(Z + Z_t)$, where Z_t is the impedance of the transmission line and $\tilde{\chi}_{AA}$ is defined in Eq. (12). The real part of Z has peaks located at frequencies where $\det\hat{M} = 0$ showing that the resonant modes can be detected by measuring the impedance or the microwave reflection rate.

The microwave absorption rate W, defined as $W = 1 - |r|^2$, is shown in Fig. 3(a). W is hugely enhanced at the frequencies of the resonance modes. An avoided crossing occurs due to linear coupling when the LC frequency matches the Higgs frequency. We find that the low-frequency mode is a well-defined mode with a frequency below the quasiparticle continuum, whereas the high-frequency mode is ill defined and decays into quasiparticle excitations, especially when $\Omega \gtrsim 2\Delta_0$. Figure 3(b) shows the modified pair susceptibility $\chi^m_{\Delta\Delta} = \hat{M}^{-1}(1,1)$, obtained by eliminating V from Eq. (13). The low-frequency mode has a significant Higgs component, especially when $LC < 1/(2\Delta_0)^2$ and the mode occurs below the quasiparticle continuum.

Figure 4 shows how the spectral weight of the Higgs mode (pair susceptibility) depends on the capacitance C of the LC circuit, with fixed LC frequency Ω_{LC}. One can see how the pair susceptibility goes from a $\sqrt{2\Delta_0 - \Omega}$ behavior in the absence of the LC mode, to a sharp resonance when coupled to the LC mode. The Higgs frequency is reduced with decreasing value of C.

The suggested experiment can be realized, for example, by galvanically coupling a 2D superconductor with strong SOC to a coplanar superconducting resonator [51]. The size of the latter can be adjusted to be in resonance with the Higgs mode. Ideally, to avoid extra damping, the Higgs frequency $2\Delta_{HM}$ of the 2D superconductor needs to be smaller than the gap of the superconductor forming the resonator. Strong SOC can also be found at the $LaAlO_3/SrTiO_3$ interface. In this case $\Delta_{HM} \sim 0.03$ meV [52], which corresponds to a bare Higgs mode frequency of around 10 GHz. This frequency is accessible with state-of-the-art microwave measurement setups. For the needed Zeeman field, $\sim 0.3\Delta_{HM}$, one can either apply an in-plane field of 0.3 T or utilize the magnetic proximity effect from an adjacent ferromagnetic insulator like EuS [53,54]. Recently, clean $LaAlO_3/SrTiO_3$ samples have been made with mobility of 19 380 cm^2/V s [55], corresponding to a scattering time of $1/\tau \approx 0.05$ meV comparable with Δ_0, which is in the parameter regime where the Higgs mode strongly couples to electromagnetic fields according to Fig. 2. Other candidate materials for the study of the effects discussed here are two-dimensional superconducting materials grown with state-of-the-art techniques in an inert atmosphere, in which the mobility, and thus the mean free path, can be increased by orders of magnitude [56]. Finally, noncentrosymmetric superconductors [38], especially those at the clean limit [57], could be potential candidates for studying the linear coupling discussed here if it were feasible to produce them as thin films.

Conclusion. We have shown that the linear Higgs-light coupling exists in a helical superconductor even without a supercurrent. From a phenomenological Ginzburg-Landau theory, we demonstrate that this linear Higgs-light coupling relies on the terms in the action related to the Lifshitz invariant. We confirm this result by explicitly calculating the susceptibility $\chi_{A\Delta}$ of a helical superconductor within a microscopic theory. We find that $\chi_{A\Delta}$ reaches its maximum at a weak disorder but vanishes in both clean and diffusive limits. We propose to reduce the mass of the Higgs mode by coupling it with an LC resonator. We demonstrate that the Higgs mode becomes an undamped regular collective mode when its frequency is reduced below the quasiparticle excitation energy $2\Delta_0$.

The linear Higgs-light coupling can show up in a system with a Lifshitz invariant. It may therefore be relevant also in the superconducting state of (twisted) multilayer graphene systems where the role of spin is replaced by the valley degree of freedom [58,59]. On the other hand, it would be interesting to study this mechanism in multiband superconductors, where it might allow for a direct visualization of the amplitude modes.

Acknowledgments. We acknowledge discussions with Miguel M. Ugeda. Y.L. and F.S.B. acknowledge financial support from the Spanish AEI through Projects PID2020-114252GB-I00 (SPIRIT), and TED2021-130292B-C42, the Basque Government through Grant No. IT-1591-22 and the IKUR strategy program. F.S.B. also acknowledges the A. v. Humboldt Foundation. R.O. was supported by the Deutsche Forschungsgemeinschaft (DFG, German Research Foundation), TRR 288, 422213477 (Project No. A07). T.T.H. was supported by the Research Council of Finland (Projects No. 317118 and 354735). The work of T.T.H., F.S.B., and S.I. WAS partially funded by the European Union's Horizon research and innovation program under Grant Agreement No. 800923 (SUPERTED project). F.S.B. thanks Prof. Björn Trauzettel and his group for their kind hospitality during his stay in Würzburg University.

[1] P. W. Higgs, Broken symmetries and the masses of gauge bosons, Phys. Rev. Lett. **13**, 508 (1964).

[2] I. Kulik, O. Entin-Wohlman, and R. Orbach, Pair susceptibility and mode propagation in superconductors: A microscopic approach, J. Low Temp. Phys. **43**, 591 (1981).

[3] A. Pashkin and A. Leitenstorfer, Particle physics in a superconductor, Science **345**, 1121 (2014).

[4] P. B. Littlewood and C. M. Varma, Gauge-invariant theory of the dynamical interaction of charge density waves and superconductivity, Phys. Rev. Lett. **47**, 811 (1981).

[5] P. B. Littlewood and C. M. Varma, Amplitude collective modes in superconductors and their coupling to charge-density waves, Phys. Rev. B **26**, 4883 (1982).

[6] M.-A. Méasson, Y. Gallais, M. Cazayous, B. Clair, P. Rodiere, L. Cario, and A. Sacuto, Amplitude Higgs mode in the $2H$-$NbSe_2$ superconductor, Phys. Rev. B **89**, 060503(R) (2014).

[7] R. Grasset, Y. Gallais, A. Sacuto, M. Cazayous, S. Mañas-Valero, E. Coronado, and M.-A. Méasson, Pressure-induced collapse of the charge density wave and Higgs mode visibility in $2H$-TaS_2, Phys. Rev. Lett. **122**, 127001 (2019).

[8] R. Grasset, T. Cea, Y. Gallais, M. Cazayous, A. Sacuto, L. Cario, L. Benfatto, and M.-A. Méasson, Higgs-mode radiance and charge-density-wave order in $2H$-$NbSe_2$, Phys. Rev. B **97**, 094502 (2018).

[9] T. Cea and L. Benfatto, Nature and Raman signatures of the Higgs amplitude mode in the coexisting superconducting and charge-density-wave state, Phys. Rev. B **90**, 224515 (2014).

[10] R. Matsunaga, Y. I. Hamada, K. Makise, Y. Uzawa, H. Terai, Z. Wang, and R. Shimano, Higgs amplitude mode in the BCS superconductors $Nb_{1-x}Ti_xN$ induced by terahertz pulse excitation, Phys. Rev. Lett. **111**, 057002 (2013).

[11] R. Matsunaga, N. Tsuji, H. Fujita, A. Sugioka, K. Makise, Y. Uzawa, H. Terai, Z. Wang, H. Aoki, and R. Shimano, Light-induced collective pseudospin precession resonating with Higgs mode in a superconductor, Science **345**, 1145 (2014).

[12] M. Beck, I. Rousseau, M. Klammer, P. Leiderer, M. Mittendorff, S. Winnerl, M. Helm, G. N. Gol'tsman, and J. Demsar, Transient increase of the energy gap of superconducting NbN thin films excited by resonant narrow-band terahertz pulses, Phys. Rev. Lett. **110**, 267003 (2013).

[13] M. Silaev, Nonlinear electromagnetic response and Higgs-mode excitation in BCS superconductors with impurities, Phys. Rev. B **99**, 224511 (2019).

[14] M. A. Silaev, R. Ojajärvi, and T. T. Heikkilä, Spin and charge currents driven by the Higgs mode in high-field superconductors, Phys. Rev. Res. **2**, 033416 (2020).

[15] R. Matsunaga, N. Tsuji, K. Makise, H. Terai, H. Aoki, and R. Shimano, Polarization-resolved terahertz third-harmonic generation in a single-crystal superconductor NbN: Dominance of the Higgs mode beyond the BCS approximation, Phys. Rev. B **96**, 020505(R) (2017).

[16] N. Tsuji and H. Aoki, Theory of Anderson pseudospin resonance with Higgs mode in superconductors, Phys. Rev. B **92**, 064508 (2015).

[17] T. Cea, C. Castellani, and L. Benfatto, Nonlinear optical effects and third-harmonic generation in superconductors: Cooper pairs versus Higgs mode contribution, Phys. Rev. B **93**, 180507(R) (2016).

[18] Y. Murotani and R. Shimano, Nonlinear optical response of collective modes in multiband superconductors assisted by nonmagnetic impurities, Phys. Rev. B **99**, 224510 (2019).

[19] N. Tsuji, Y. Murakami, and H. Aoki, Nonlinear light–Higgs coupling in superconductors beyond BCS: Effects of the retarded phonon-mediated interaction, Phys. Rev. B **94**, 224519 (2016).

[20] G. Seibold, M. Udina, C. Castellani, and L. Benfatto, Third harmonic generation from collective modes in disordered superconductors, Phys. Rev. B **103**, 014512 (2021).

[21] N. Tsuji and Y. Nomura, Higgs-mode resonance in third harmonic generation in NbN superconductors: Multiband electron-

phonon coupling, impurity scattering, and polarization-angle dependence, Phys. Rev. Res. **2**, 043029 (2020).
[22] A. Moor, A. F. Volkov, and K. B. Efetov, Amplitude Higgs mode and admittance in superconductors with a moving condensate, Phys. Rev. Lett. **118**, 047001 (2017).
[23] A. Volkov and S. M. Kogan, Collisionless relaxation of the energy gap in superconductors, Sov. Phys. JETP **38**, 1018 (1974).
[24] D. Sherman, U. S. Pracht, B. Gorshunov, S. Poran, J. Jesudasan, M. Chand, P. Raychaudhuri, M. Swanson, N. Trivedi, A. Auerbach *et al.*, The Higgs mode in disordered superconductors close to a quantum phase transition, Nat. Phys. **11**, 188 (2015).
[25] T. Cea, C. Castellani, G. Seibold, and L. Benfatto, Nonrelativistic dynamics of the amplitude (Higgs) mode in superconductors, Phys. Rev. Lett. **115**, 157002 (2015).
[26] D. Agterberg, Novel magnetic field effects in unconventional superconductors, Physica C: Superconductivity **387**, 13 (2003).
[27] R. P. Kaur, D. F. Agterberg, and M. Sigrist, Helical vortex phase in the noncentrosymmetric $CePt_3Si$, Phys. Rev. Lett. **94**, 137002 (2005).
[28] O. Dimitrova and M. V. Feigel'man, Theory of a two-dimensional superconductor with broken inversion symmetry, Phys. Rev. B **76**, 014522 (2007).
[29] A. Buzdin, Direct coupling between magnetism and superconducting current in the Josephson φ_0 junction, Phys. Rev. Lett. **101**, 107005 (2008).
[30] F. S. Bergeret and I. V. Tokatly, Theory of diffusive φ_0 Josephson junctions in the presence of spin-orbit coupling, Europhys. Lett. **110**, 57005 (2015).
[31] F. Ando, Y. Miyasaka, T. Li, J. Ishizuka, T. Arakawa, Y. Shiota, T. Moriyama, Y. Yanase, and T. Ono, Observation of superconducting diode effect, Nature (London) **584**, 373 (2020).
[32] A. Daido, Y. Ikeda, and Y. Yanase, Intrinsic superconducting diode effect, Phys. Rev. Lett. **128**, 037001 (2022).
[33] K. Jiang and J. Hu, Superconducting diode effects, Nat. Phys. **18**, 1145 (2022).
[34] N. F. Yuan and L. Fu, Supercurrent diode effect and finite-momentum superconductors, Proc. Natl. Acad. Sci. USA **119**, e2119548119 (2022).
[35] S. Ilić and F. S. Bergeret, Theory of the supercurrent diode effect in Rashba superconductors with arbitrary disorder, Phys. Rev. Lett. **128**, 177001 (2022).
[36] J. J. He, Y. Tanaka, and N. Nagaosa, A phenomenological theory of superconductor diodes, New J. Phys. **24**, 053014 (2022).
[37] V. P. Mineev and K. V. Samokhin, Nonuniform states in noncentrosymmetric superconductors: Derivation of Lifshitz invariants from microscopic theory, Phys. Rev. B **78**, 144503 (2008).
[38] E. Bauer and M. Sigrist, *Non-Centrosymmetric Superconductors: Introduction and Overview* (Springer Science & Business Media, 2012).
[39] Note that here we only consider conventional single-band superconductors, and hence all the conclusions are drawn for a single-band superconductor. In principle, multiple-band superconductors allow for construction for another type of Lifshitz invariant with time-reversal and inversion symmetry [60,61]. However, this term does not contribute to the linear Higgs light coupling.
[40] In all models we have considered, $\mathrm{Im}(\eta^2) \leqslant 0$ and therefore the overall linewidth stays positive.
[41] M. Houzet and J. S. Meyer, Quasiclassical theory of disordered Rashba superconductors, Phys. Rev. B **92**, 014509 (2015).
[42] See Supplemental Material at http://link.aps.org/supplemental/10.1103/PhysRevB.108.224517, which includes derivations of all the susceptibilities, frequency dependence of $\chi_{A\Delta}$, the explanation of vanishing of $\chi_{A\Delta}$ in the diffusive limit, and the derivation of the equations of motion.
[43] P. J. Crowley and L. Fu, Supercurrent-induced resonant optical response, Phys. Rev. B **106**, 214526 (2022).
[44] M. Papaj and J. E. Moore, Current-enabled optical conductivity of superconductors, Phys. Rev. B **106**, L220504 (2022).
[45] The code for calculating the Higgs-field susceptibility $\chi_{h\Delta}$ will be made available at https://gitlab.jyu.fi/jyucmt/higgs-light-coupling.
[46] A. Samanta, A. Das, N. Trivedi, and R. Sensarma, Thermal effects on collective modes in disordered *s*-wave superconductors, Phys. Rev. B **105**, 104503 (2022).
[47] T. Cea, D. Bucheli, G. Seibold, L. Benfatto, J. Lorenzana, and C. Castellani, Optical excitation of phase modes in strongly disordered superconductors, Phys. Rev. B **89**, 174506 (2014).
[48] G. Seibold, L. Benfatto, and C. Castellani, Application of the Mattis-Bardeen theory in strongly disordered superconductors, Phys. Rev. B **96**, 144507 (2017).
[49] B. Fan, A. Samanta, and A. M. García-García, Characterization of collective excitations in weakly coupled disordered superconductors, Phys. Rev. B **105**, 094515 (2022).
[50] Here, we have neglected the phase mode and the plasma mode at higher frequencies much larger than $2\Delta_0$, as they do not contribute to the electric response at lower frequencies.
[51] A. Wallraff, D. I. Schuster, A. Blais, L. Frunzio, R.-S. Huang, J. Majer, S. Kumar, S. M. Girvin, and R. J. Schoelkopf, Strong coupling of a single photon to a superconducting qubit using circuit quantum electrodynamics, Nature (London) **431**, 162 (2004).
[52] N. Reyren, S. Gariglio, A. Caviglia, D. Jaccard, T. Schneider, and J.-M. Triscone, Anisotropy of the superconducting transport properties of the $LaAlO_3/SrTiO_3$ interface, Appl. Phys. Lett. **94**, 112506 (2009).
[53] P. Wei, S. Lee, F. Lemaitre, L. Pinel, D. Cutaia, W. Cha, F. Katmis, Y. Zhu, D. Heiman, J. Hone *et al.*, Strong interfacial exchange field in the graphene/EuS heterostructure, Nat. Mater. **15**, 711 (2016).
[54] E. Strambini, V. N. Golovach, G. De Simoni, J. S. Moodera, F. S. Bergeret, and F. Giazotto, Revealing the magnetic proximity effect in EuS/Al bilayers through superconducting tunneling spectroscopy, Phys. Rev. Mater. **1**, 054402 (2017).
[55] S. Gupta and B. I. Yakobson, What dictates Rashba splitting in 2D van der Waals heterobilayers, J. Am. Chem. Soc. **143**, 3503 (2021).
[56] Y. Cao, A. Mishchenko, G. Yu, E. Khestanova, A. Rooney, E. Prestat, A. Kretinin, P. Blake, M. B. Shalom, C. Woods *et al.*, Quality heterostructures from two-dimensional crystals unstable in air by their assembly in inert atmosphere, Nano Lett. **15**, 4914 (2015).
[57] H. Q. Yuan, D. F. Agterberg, N. Hayashi, P. Badica, D. Vandervelde, K. Togano, M. Sigrist, and M. B. Salamon, *s*-wave spin-triplet order in superconductors without inversion symmetry: Li_2Pd_3B and Li_2Pt_3B, Phys. Rev. Lett. **97**, 017006 (2006).
[58] J.-X. Lin, P. Siriviboon, H. D. Scammell, S. Liu, D. Rhodes, K. Watanabe, T. Taniguchi, J. Hone, M. S. Scheurer, and J.

Li, Zero-field superconducting diode effect in small-twist-angle trilayer graphene, Nat. Phys. **18**, 1221 (2022).

[59] Y.-M. Xie, D. K. Efetov, and K. Law, φ_0-Josephson junction in twisted bilayer graphene induced by a valley-polarized state, Phys. Rev. Res. **5**, 023029 (2023).

[60] T. Kamatani, S. Kitamura, N. Tsuji, R. Shimano, and T. Morimoto, Optical response of the Leggett mode in multiband superconductors in the linear response regime, Phys. Rev. B **105**, 094520 (2022).

[61] R. Nagashima, S. Tian, R. Haenel, N. Tsuji, and D. Manske, Classification of Lifshitz invariant in multiband superconductors: An application to Leggett modes in the linear response regime in kagome lattice models, arXiv:2309.01410.